

LETTERS

Spectroscopic Observation of Ion-Induced Water Dimer Dissociation in the $X^-(H_2O)_2$ ($X = F, Cl, Br, I$) Clusters

Patrick Ayotte, Steen B. Nielsen,[†] Gary H. Weddle,[‡] and Mark A. Johnson*

Sterling Chemistry Laboratory, Yale University, P.O. Box 208107, New Haven, Connecticut 06520-8107

Sotiris S. Xantheas

Environmental Molecular Sciences Laboratory, Pacific Northwest National Laboratory, P.O. Box 999, MS K8-91 Richland, Washington 99352

Received: June 15, 1999; In Final Form: October 4, 1999

We elucidate the interplay between the ion–water and water–water interactions in determining the structures of halide ion–water clusters using infrared spectroscopy, interpreted with *ab initio* theory. Vibrational predissociation spectra of the $X^-(H_2O)_2 \cdot Ar_m$ ($X = F, Cl, Br, I$) clusters in the OH stretching region (2300–3800 cm^{-1}) reveal a strongly halide-dependent pattern of bands. These spectra encode the incremental weakening of the interaction between the water molecules with the lighter halides, finally leading to their complete dissociation in the fluoride complex. A consequence of this is that the $F^-(H_2O)_2$ cluster is likely to be a floppy system with high amplitude zero point motion, in contrast to the pseudo-rigid behavior of the other halide hydrates.

I. Introduction

When anions are solvated by water, the ionic hydrogen-bonds act to either disrupt or reinforce the ambient water networks depending on the particular ion. The fluoride ion, for example, acts as a so-called “structure-maker,” reducing the entropy of water, while “structure-breakers” like iodide decrease order, suggesting a qualitative difference in the solvation morphologies for the different halides.¹ Here, we explore the fundamental motif involved in this competition between ion–water and interwater solvation by following the halide dependence of the OH stretching spectra in isolated $X^-(H_2O)_2$ clusters ($X = F,$

Cl, Br, I). Both *ab initio*^{4,5} and molecular dynamics^{6–9} treatments indicate that these clusters display a dramatic reduction in the interaction between the two waters as the ionic H-bond (IHB) strengths are systematically increased from iodide to chloride,^{10–15} finally resulting in nearly complete dissociation of the interwater H-bond in the fluoride complex.^{16–20} We note that there is a recent cluster study by Cabarcos et al.,²¹ which reported the dissociation of the water trimer upon complexation with fluoride. However, as we discuss below, the $F^-(H_2O)_3$ ensemble used in that study left open the question of whether the network was thermally broken apart or whether this dissociation reflected an intrinsic property of the potential surface. In this work, we quench the $X^-(H_2O)_2$ parent cluster ions close to their minimum energy structures by complexation with argon atoms^{2,3} and illustrate the power of this method by reporting the first observation of interwater bonding in the $Cl^-(H_2O)_2$ and

* Corresponding author. TEL: 203-432-5226. FAX: 203-432-6144. Email: mark.johnson@yale.edu.

[†] Also at Department of Chemistry, University of Copenhagen, The H.C. Ørsted Institute, DK- 2100 København Ø, Denmark.

[‡] Present address: Department of Chemistry, Fairfield University, Fairfield, Connecticut 06430.

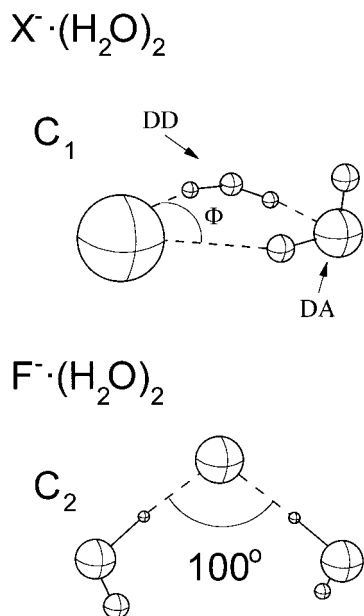


Figure 1. Schematic structure of the C_1 isomer (adopted by $X = I, Br,$ and Cl) and the calculated (MP2/aug-cc-pVTZ level) minimum energy (C_2) geometry of $F^-(H_2O)_2$. For the C_1 form, one water acts as a double-donor (DD) and the other as a donor-acceptor (DA), while they are symmetric in the C_2 structure.

$Br^-(H_2O)_2$ systems in accordance with earlier theoretical predictions.^{5,15}

This work builds on previous experimental and theoretical results from our laboratories^{2,3,5,15-17} on the structural and spectral patterns of the first few halide-water clusters. That work provides the assignments of specific features in the spectrum of the $I^-(H_2O)_2$ complex to OH stretch fundamentals in particular H-bonding environments within the cyclic (C_1) network illustrated in Figure 1. In this configuration, the two water molecules are distinguishable according to the interwater H-bond topology, with one water adopting a double-donor (DD) arrangement and the other acting as a donor-acceptor (DA). Here we capitalize on these assignments to determine how ionic and interwater interactions compete in the halide hydrates.

II. Experimental and Theoretical Approaches

The dramatic reduction anticipated in the intracuster dissociation energies of the networked water molecules in the $X^-(H_2O)_2$ complexes (calculated to be only ~ 60 cm^{-1} for the water-water bond energy in $Cl^-(H_2O)_2$, including zero-point energy corrections)^{5,15} compared to that of the bare water dimer [$D_0(H_2O-H_2O) \sim 1260$ cm^{-1}]²²⁻²⁶ necessitates working with very cold cluster ions in order to quench the systems into these shallow minima. This problem is exacerbated in the light halides^{21,27} because their increasing monomer evaporation energies (i.e., $\Delta H_{1,2}[X^-(H_2O)_2 \rightarrow X^- \cdot H_2O + H_2O] \approx 3320, 4060, 4550,$ and 6720 cm^{-1} for $X = I, Br, Cl,$ and $F,$ respectively)¹¹ lead to larger internal energy content in the $X^-(H_2O)_2$ cluster ion distributions.²⁸ Compounding the problem, the OH stretching transitions in the lighter halide complexes red shift relative to those in $I^-(H_2O)_2$, so that the internal excitation upon photon absorption falls incrementally even farther below their respective water evaporation thresholds. These effects conspire to frustrate the extension of linear action spectroscopy (as was used to study the iodide hydrates)²⁹ to the smaller halides.

Fortunately, we have recently demonstrated argon predissociation spectroscopy:^{2,3,30,31}

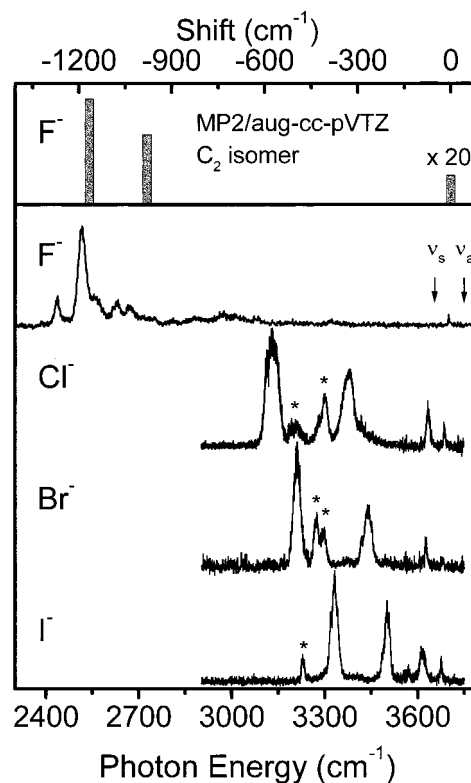
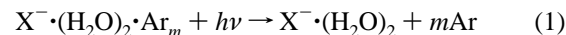


Figure 2. Vibrational spectra of the $X^-(H_2O)_2 \cdot Ar_3$ clusters recorded by argon predissociation into $X^-(H_2O)_2$. The top panel is the MP2/aug-cc-pVTZ (harmonic) spectrum of the C_2 isomer of $F^-(H_2O)_2$, displayed as the shift from the mean of the symmetric and asymmetric stretches (labeled ν_s and ν_a) in water vapor.



to be an effective means of characterizing weakly bound networks, where the argons serve to both limit the internal energy content of the $X^-(H_2O)_2$ complex and enable detection (via action spectroscopy) of low energy spectral features without requiring multiphoton excitation. We report spectra for $m = 3$, which yields the best compromise between large parent intensity and small background from collision-induced and metastable dissociation. Note, however, that the spectra were recorded for $m = 1-3$ to ensure that the observed patterns do not depend on the extent of argon solvation.

Spectra were obtained using a tandem time-of-flight photo-fragmentation spectrometer described in detail previously,³² where excitation is carried out at the transient focus of the first spectrometer with a pulsed infrared laser (Laser Vision, KTA/KTP optical parametric oscillator, ~ 2 mJ/pulse, bandwidth ~ 2 cm^{-1}). The resulting action spectra were normalized to fluctuations in laser pulse energy.

First principles ab initio calculations were performed at the second-order Møller-Plesset perturbation level of theory (MP2) using the correlation consistent polarized valence basis sets of double (aug-cc-pVDZ) and triple (aug-cc-pVTZ) ζ quality.³³ To assess the structural and spectral implications of the Ar atom on the clusters, we also performed ab initio calculations for the $F^-(H_2O)_2 \cdot Ar$ system with the singly and doubly augmented correlation consistent set (d-aug-cc-pVDZ) for Ar.³⁴

III. Results and Discussion

III. A. Appearance of the Spectra. Figure 2 presents the mid-IR argon predissociation spectra of the $X^-(H_2O)_2 \cdot Ar_3$ clusters. The lower trace displays the previously reported^{2,3}

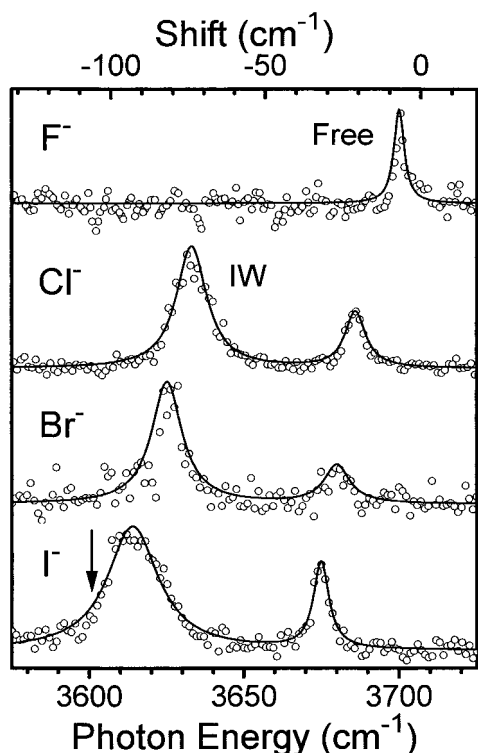


Figure 3. Expanded view of the $X^- \cdot (H_2O)_2$ higher energy modes. The arrow indicates the position of the interwater H-bonded OH stretch fundamental observed in the neutral water dimer.^{38,39} Band labels correspond to IW = interwater H-bonded, and Free = free OH stretches.

spectrum from $I^- \cdot (H_2O)_2 \cdot Ar_3$, with the characteristic pattern of four fundamentals expected from the H-bonded (C_1) structure shown in Figure 1 (the band marked (*) is assigned to the $2 \leftarrow 0$ overtone of the intramolecular bend, as discussed below). This pattern evolves smoothly from I^- to Cl^- but changes dramatically at F^- , where the most intense band shifts abruptly by an additional 600 cm^{-1} to the red. First, we discuss the slow evolution from iodide to chloride in the context of our previous work on the halide dependence of the $X^- \cdot H_2O$ monohydrates³⁰ and the assignments of the $I^- \cdot (H_2O)_2$ spectrum.^{2,3}

III. B. Weakening of the Interwater H-Bond in the $I^- \cdot (H_2O)_2$, $Br^- \cdot (H_2O)_2$, and $Cl^- \cdot (H_2O)_2$ Series. Qualitatively, there are two main classes of bands in the I^- , Br^- , and Cl^- series, distinguishable by their halide dependence, such that the basic four-band pattern in $I^- \cdot (H_2O)_2$ splits apart in going to smaller halides. Two simple bands appear on the high-energy side ($> 3600 \text{ cm}^{-1}$), which weakly blue shift up the halide series (see Figure 3), while the bands at lower energy ($\leq 3500 \text{ cm}^{-1}$) are more complex and generally display a red-shift from I^- to Cl^- . The two most intense bands in $I^- \cdot (H_2O)_2$ [at 3331 and 3500 cm^{-1}] arise from the two ionic H-bonded OH stretches (OH_{IHB}) of the DD and DA waters, with the DA water displaying the larger red-shift and intensity. The band associated with the free OH (OH_{Free}) on the DA water appears as the weak feature around 3680 cm^{-1} , resonating closest to the mean energy ($\nu_0 = 3707 \text{ cm}^{-1}$) of the two OH stretches in bare water (3657 and 3756 cm^{-1} for the symmetric and asymmetric modes, labeled ν_s and ν_a in the upper trace of Figure 2). The remaining band at 3616 cm^{-1} is associated with the interwater, H-bonded OH stretch (OH_{IW}) on the DD water. The large splitting (344 cm^{-1}) between the IHB and free OH stretches of the DA water indicates that these modes correspond to local oscillators, while the two OH stretches on the DD water are more collective in nature.²

The red shift of the OH_{IHB} bands displayed by the lighter $X^- \cdot (H_2O)_2$ complexes (Figure 2) reflects the general trend established in the $X^- \cdot H_2O$ monohydrates ($X = Cl, Br, \text{ and } I$),³⁰ where we observed an approximately quadratic dependence³⁵ of the red shift ($\Delta\nu = \nu_0 - \nu_{IHB}$) on the ionic H-bond strength, characterized by the thermochemically determined enthalpies of hydration $\Delta H_{0,1}$.^{10–14} In general, both (DA and DD) OH_{IHB} bands of the dihydrates red-shift by $40\text{--}70 \text{ cm}^{-1}$ for each halide. There is obviously increasing complexity of these OH_{IHB} bands, however, which precludes the application of such a simple rule to extract effective ionic H-bond strengths. Similar complexity was observed³⁰ in the monohydrates (as well as in the $X^- \cdot (H_2O)_3$ series),³¹ where it was assigned to the Fermi interactions between the OH_{IHB} stretch and the $2 \leftarrow 0$ overtone of the HOH bend ($H_{Fermi} \approx 30 \text{ cm}^{-1}$). Basically, the energies of the bend overtones ($2\nu_2 = 3151 \text{ cm}^{-1}$ in water vapor) are not strongly halide dependent, while the location of the OH_{IHB} stretches red shift dramatically as the ionic H-bonds become stronger, accidentally “tuning” into resonance when they occur in the $3200\text{--}3300 \text{ cm}^{-1}$ range. Thus, the relatively simple pattern observed for $I^- \cdot (H_2O)_2$, with a weak bend overtone band at 3228 cm^{-1} , evolves into six bands in the $Cl^- \cdot (H_2O)_2$ and $Br^- \cdot (H_2O)_2$ systems, as the two OH_{IHB} stretching fundamentals interact with their respective bend overtones, causing perturbed band positions and strong “extra” bands. It is also conceivable that the OH_{IHB} excitations involve proton-transfer processes in the vibrational excited states^{36,37} with more basic halides, and we postpone further treatment of that problem until higher resolution spectra become available.

While the OH_{IHB} stretches strongly red-shift in response to the increased ionic interaction in the lighter halide complexes, the two high-frequency modes OH_{IW} and OH_{Free} display a comparatively smaller blue-shift. When combined with the red-shifting OH_{IHB} bands, however, the overall effect is a dramatic opening of the gap between the two double-donor modes. This larger splitting implies increasingly localized excitations as the intramolecular coupling matrix element (in bare water) is only about 50 cm^{-1} . Thus, while the DD modes are collective² in $I^- \cdot (H_2O)_2$, they are much better characterized as local OH_{IHB} and OH_{IW} excitations in $Cl^- \cdot (H_2O)_2$.⁵ This implies that the high energy bands provide a clean diagnostic for the extent of solvent networking, just as the low energy bands encode the ion–water interaction.³¹

We follow the evolution of the OH_{IW} stretch bands with the expanded view in Figure 3. The arrow in the lower trace of this figure indicates the frequency of the OH_{IW} stretch in the bare water dimer,^{24,25,38,39} which falls surprisingly close to the observed OH_{IW} feature in $I^- \cdot (H_2O)_2$.^{2,3} The blue shift of the OH_{IW} band in the lighter halide complexes³¹ reflects the anticipated weakening in the $H_2O\text{--}H_2O$ interaction: as the water molecules separate [i.e., $\Phi = 48^\circ, 53^\circ, \text{ and } 57^\circ$ for I^- , Br^- and Cl^- , respectively, where Φ denotes the calculated O–X–O angle (see Figure 1)],^{2,5} the OH_{IW} band blue shifts toward the OH_{Free} band. In this context, the increasing splitting between the OH_{IHB} and OH_{IW} bands in the DD water can be traced to strengthening of the ionic H-bonds and concomitant weakening of the interwater H-bond. Apparently, the stronger ionic H-bonds lead to a more linear $X^- \cdots H\text{--}O$ arrangement,^{5,16} which, in turn, destabilizes the directional $O \cdots H\text{--}O$ interaction.⁴⁰

III. C. Dissociation of the Water Dimer in the $F^- \cdot (H_2O)_2$ Cluster. The $F^- \cdot (H_2O)_2$ spectrum (top trace in Figure 2) is clearly distinct from the other halogens, with a dominant OH_{IHB} band at 2520 cm^{-1} and only a single sharp feature in the location of OH_{Free} (see expanded view in Figure 3 and Table 1 for band

TABLE 1: Observed Band Positions in the $X^-(\text{H}_2\text{O})_2\cdot\text{Ar}_3$ Complexes

	assignment	band position ($\pm 2 \text{ cm}^{-1}$)
$\text{I}^-(\text{H}_2\text{O})_2\cdot\text{Ar}_3$	$2\nu_2$	3228
	IHB	3331, 3500
	IW	3616
	free	3675
$\text{Br}^-(\text{H}_2\text{O})_2\cdot\text{Ar}_3$	$2\nu_2$	3267, 3290
	IHB	3207, 3438
	IW	3625
	free	3680
$\text{Cl}^-(\text{H}_2\text{O})_2\cdot\text{Ar}_3$	$2\nu_2$	3202, 3301
	IHB	3130, 3375
	IW	3633
	free	3686
$\text{F}^-(\text{H}_2\text{O})_2\cdot\text{Ar}_3$	IHB	(2435), 2520
	free	3700

positions). The shift [$v_o - v_{\text{free}} \sim 7 \text{ cm}^{-1}$] is the smallest in the series. Note the conspicuous absence of absorption in the vicinity of the strong OH_{IW} bands present in the heavier halides. This indicates that the water molecules have effectively dissociated in the $\text{F}^-(\text{H}_2\text{O})_2$ cluster. A similar structural motif was recently reported for the clusters of fluoride with 3–5 water molecules, although the evaporative ensemble used to acquire those spectra would not have explored delicate networked structures, if present.²¹ While the lower $\text{F}^-\cdot\text{Ar}$ binding energy ($\sim 1100 \text{ cm}^{-1}$)⁴¹ reduces the internal energy content in hot ensembles of $\text{F}^-(\text{H}_2\text{O})_2$ by almost a factor of 10, it is, of course, possible that this residual energy is causing the break-up of a very weakly bound water dimer. The spectra of networked waters are quite distinct from the thermally induced open structures in the other halide hydrates,^{21,27,29} and indeed we have observed² large changes in the spectra of those complexes as the dimers are quenched into their shallow networked minima. Since we observe that the $\text{F}^-(\text{H}_2\text{O})_2\cdot\text{Ar}_m$ spectra do not change with sequential argon solvation (for $m = 1-3$, data not shown), we argue against a thermal break-up as the cause for the loss of interwater binding, and we suggest that the effect arises from an intrinsic feature of the surface.

The breaking apart of the dimer bond in the $\text{F}^-(\text{H}_2\text{O})_2$ system has been anticipated by previous first principles calculations^{16,18} and again at the MP2/aug-cc-pVTZ level of theory (presented here). The minimum on the electronic energy surface has C_2 symmetry with an O–F–O angle of 100° as displayed in Figure 1 [consistent with Kim’s analysis¹⁸ using a density functional (BeckeLYP/6-311++G**) approach]. The calculated spectrum for the C_2 structure (MP2/aug-cc-pVTZ) is displayed at the top of Figure 2. This indeed recovers the gross features in the observed spectrum, with a weak, sharp band near zero shift, and a much more intense band corresponding to the out-of-phase vibration of the OH_{IHB} stretches, which is red shifted by 1167 cm^{-1} . The residual splitting in the OH_{Free} band is calculated to be quite small ($< 1 \text{ cm}^{-1}$), accounting for the presence of only one sharp band at 3700 cm^{-1} in the $\text{F}^-(\text{H}_2\text{O})_2$ spectrum (Figure 3) at our present resolution of $\sim 2 \text{ cm}^{-1}$. On the other hand, a second, intense OH_{IHB} band, which arises from the in-phase OH_{IHB} vibration, is calculated to occur with a red shift of 980 cm^{-1} , but is not evident in the spectrum. This apparent disagreement can be reconciled, however, when one considers the floppy nature of the surface. The planar, symmetrical structure with C_{2h} symmetry ($\Phi = 180^\circ$), for example, is a first-order transition state, lying 120 cm^{-1} above the C_2 minimum, which results in a barrier of only about 6 cm^{-1} after harmonic zero-point correction. Thus, we expect a very flat surface when varying the angle between the (three) heavy atoms from 100 to 180° . As this high amplitude motion does not explore arrange-

ments in which there is significant H-bonding between the two water molecules, all such structures yield a sharp OH_{Free} feature. The OH_{IHB} band intensities are more sensitive to structure than the OH_{Free} , however, as the calculated weaker in-phase OH_{IHB} band of the C_2 isomer (at -980 cm^{-1} shift) becomes symmetry forbidden in the C_{2h} form, while the position and intensity of the strong band are relatively unaffected (red-shifted by 1167 vs 1135 cm^{-1} for the C_2 and C_{2h} isomers, respectively). Note that previous calculations^{16,18} with smaller basis sets and/or lower levels of theory underestimated the magnitude of this shift by about 100 cm^{-1} .

The flatness of the surface suggests that the observed bands may result from averaging over many bent configurations, even at the zero point. These considerations lead us to conclude that while the heavier $X^-(\text{H}_2\text{O})_2$ systems behave like quasi-rigid systems, where the spectra indeed reflect the curvature of the global minima in their potential surfaces, the $\text{F}^-(\text{H}_2\text{O})_2$ system is likely to be more akin to floppy (neutral) van der Waals complexes, where the spectra bear a more distant relationship to the harmonic frequencies about a single point on the surface. At present, the existence of many unassigned weak bands in the OH_{IHB} range precludes definitive assignment of structure, and they may arise from residual energy in the clusters, combination bands with soft modes, or the presence of multiple isomers. (Note that the spectroscopic signatures of both the H-bonded and the open isomers were simultaneously observed in the (hot) $\text{I}^-(\text{H}_2\text{O})_2$ complex.)²

Finally, we have considered the effect that the Ar atom has on the structure and spectra of the $\text{F}^-(\text{H}_2\text{O})_2$ cluster by explicitly incorporating it into the ab initio calculations. Our goal was to investigate whether it induces any particular structural effects, for instance by inserting between the water molecules and therefore altering the nearly free motion between the C_2 and C_{2h} arrangements previously discussed for the bare $\text{F}^-(\text{H}_2\text{O})_2$ cluster. For the weakly bound $\text{Ar}\cdot\text{H}_2\text{O}$ system, previous studies⁴² suggested that the Ar atom moves freely from the H-bridged structure to another coplanar arrangement with a nearly perpendicular orientation between the C_2 (water) and Ar–O axes. Starting from various different arrangements in the $\text{F}^-(\text{H}_2\text{O})_2\cdot\text{Ar}$ cluster (e.g., chosen to probe these H-bridged vs lone pair bonding scenarios) we have found that they all collapse to a single minimum energy structure where the Ar atom forms a pyramid with the other three heavy atoms. (The O–(F–Ar–O) dihedral angle is 93.6° .) The minimum energy geometry has no symmetry since the two water molecules are rotated from their C_2 positions in order to accommodate simultaneous weak H-bridge and lone pair alignments between the Ar atom and the two water molecules. However, the O–F–O angle and O–O distance are only changed by $< 0.1^\circ$ and $< 0.001 \text{ \AA}$, respectively, with respect to their values in the bare $\text{F}^-(\text{H}_2\text{O})_2$ cluster, indicating that the argon induces very little perturbation in the interwater H-bonding character. Another indication that the shape of the $\text{F}^-(\text{H}_2\text{O})_2$ surface is intact upon argon solvation is the fact that the corresponding “breathing” modes which mediate interconversion between the C_2 and C_{2h} arrangements (in the $310-330 \text{ cm}^{-1}$ range) change less than 1 cm^{-1} in the argon complex. The two OH_{IHB} bands are calculated to red shift by 7 and 15 cm^{-1} , respectively, upon complexation with the weakly bound Ar atom (similar to our experimental observations for the sequential argon shift), and the lower symmetry of the complex causes the very small ($< 1 \text{ cm}^{-1}$) spacing between the OH_{Free} modes to increase to about 10 cm^{-1} . We do not observe this splitting in the $\text{F}^-(\text{H}_2\text{O})_2\cdot\text{Ar}_3$ cluster, which was the smallest argon cluster for which we could get sufficient signal-

to-noise to clearly express the very weak OH_{free} feature. The observed single line in that cluster may arise from the multiple argons, perhaps occupying symmetrical sites. Before drawing conclusions, however, we caution that the ab initio approach represents the most extreme situation where the argon-solvated fluoride dihydrate is quenched to the minimum in the potential, while our F⁻·(H₂O)₂·Ar ensemble is evaporative with respect to argon, and therefore displays large amplitude motion of the most weakly bound species. The calculations presented here are therefore expected to overestimate the perturbative effect of the Ar atom, which may well be washed out upon inclusion of the large amplitude motion at the zero point.

IV. Conclusion

The OH stretching spectra previously observed for the I⁻·(H₂O)₂ complex evolve smoothly in Br⁻·(H₂O)₂ and Cl⁻·(H₂O)₂, indicating an incremental weakening of the interwater H-bond. The fluoride complex, however, displays very strongly red-shifted OH_{IHB} stretches as well as a single feature at 3700 cm⁻¹, the expected pattern to occur when the interwater H-bond is effectively broken. Thus, the strong fluoride-water bond overtakes the inter-water interaction to become the uniquely “internally” solvated species among the halides.

Acknowledgment. We thank the National Science Foundation, Experimental Physical Chemistry Division, for support of this work. P.A. acknowledges support from FCAR. Part of this work was performed under the auspices of the Division of Chemical Sciences, Office of Basic Energy Sciences, U.S. Department of Energy under Contract DE-AC06-76RLO 1830 with Battelle Memorial Institute, which operates the Pacific Northwest National Laboratory. Computer resources were provided by the Division of Chemical Sciences and by the Scientific Computing Staff, Office of Energy Research, at the National Energy Research Supercomputer Center (Berkeley, CA).

References and Notes

- (1) Marcus, Y. *Ion Solvation*; Wiley-Interscience: Chichester, 1985.
- (2) Ayotte, P.; Weddle, G. H.; Kim, J.; Johnson, M. A. *Chem. Phys.* **1998**, *239*, 485.
- (3) Ayotte, P.; Weddle, G. H.; Kim, J.; Kelley, J. A.; Johnson, M. A. *J. Phys. Chem. A* **1999**, *103*, 443.
- (4) Combariza, J. E.; Kestner, N. R.; Jortner, J. *J. Chem. Phys.* **1994**, *100*, 2851.
- (5) Xantheas, S. S.; *J. Phys. Chem.* **1996**, *100*, 9703.
- (6) Perera, L.; Berkowitz, M. L. *J. Chem. Phys.* **1993**, *99*, 4222.
- (7) Perera, L.; Berkowitz, M. L. *J. Chem. Phys.* **1994**, *100*, 3085.
- (8) Sung, S.-S.; Jordan, P. C. *J. Chem. Phys.* **1986**, *85*, 4045.
- (9) Lin, S.; Jordan, P. C. *J. Chem. Phys.* **1988**, *89*, 7492.
- (10) Arshadi, M.; Yamadagni, R.; Kebarle, P. *J. Phys. Chem.* **1970**, *74*, 1475.
- (11) Hiraoka, K.; Mizuse, S.; Yamabe, S. *J. Phys. Chem.* **1988**, *92*, 3943.
- (12) Keesee, R. G.; Castleman, A. W., Jr. *Chem. Phys. Lett.* **1980**, *74*, 139.
- (13) Keesee, R. G.; Castleman, A. W., Jr. *J. Phys. Chem. Ref. Data* **1986**, *15*, 1011.
- (14) Weis, P.; Kemper, P. R.; Bowers, M. T.; Xantheas, S. S.; *J. Am. Chem. Soc.* **1999**, *121*, 3531.
- (15) Dorsett, H. E.; Watts, R. O.; Xantheas, S. S. *J. Phys. Chem. A* **1999**, *103*, 3351.
- (16) Xantheas, S. S.; T. H. Dunning Jr., *J. Phys. Chem.* **1994**, *98*, 13489.
- (17) Xantheas, S. S.; Dang, L. X. *J. Phys. Chem.* **1996**, *100*, 3989.
- (18) Baik, J.; Kim, J.; Majumdar, D.; Kim, K. S. *J. Chem. Phys.* **1999**, *110*, 9116.
- (19) Combariza, J. E.; Kestner, N. R. *J. Phys. Chem.* **1994**, *98*, 3513.
- (20) Bryce, R. A.; Vincent, M. A.; Malcolm, N. O. J.; Hillier, I. H.; Burton, N. A. *J. Chem. Phys.* **1998**, *109*, 3077.
- (21) Cabarcos, O. M.; Weinheimer, C. J.; Xantheas, S. S.; Lisy, J. M. *J. Chem. Phys.* **1999**, *110*, 5.
- (22) Curtis, L. A.; Frurip, D. J.; Blander, M. *J. Chem. Phys.* **1979**, *71*, 2703.
- (23) Honegger, E.; Leutwyler, S. *J. Chem. Phys.* **1988**, *88*, 2582.
- (24) Xantheas, S. S.; Dunning, T. H., Jr. *J. Chem. Phys.* **1994**, *99*, 8774.
- (25) Fredericks, S. E.; Jordan, K. D.; Zwier, T. S. *J. Phys. Chem.* **1996**, *100*, 7810.
- (26) Feyereisen, M. W.; Feller, D.; Dixon, D. A. *J. Phys. Chem.* **1996**, *100*, 2993.
- (27) Choi, J.-H.; Kuwata, K. T.; Cao, Y.-B.; Okumura, M. *J. Phys. Chem. A* **1998**, *102*, 503.
- (28) Klots, C. E.; *J. Chem. Phys.* **1985**, *83*, 5854.
- (29) Ayotte, P.; Bailey, C. G.; Weddle, G. H.; Johnson, M. A. *J. Phys. Chem. A* **1998**, *102*, 3067.
- (30) Ayotte, P.; Weddle, G. H.; Kim, J.; Johnson, M. A. *J. Am. Chem. Soc.* **1998**, *120*, 12361.
- (31) Ayotte, P.; Weddle, G. H.; Johnson, M. A. *J. Chem. Phys.* **1999**, *110*, 7129.
- (32) Johnson, M. A.; Lineberger, W. C. In *Techniques for the Study of Gas-Phase Ion Molecule Reactions*; Farrar, J. M., Saunders, W., Eds.; Wiley: New York, 1988; p 591.
- (33) Dunning, T. H., Jr. *J. Chem. Phys.* **1989**, *90*, 1007; Kendall, R. A.; Dunning, T. H., Jr.; Harrison, R. J. *J. Chem. Phys.* **1992**, *96*, 6796.
- (34) Woon, D. E.; Dunning, T. H., Jr. *J. Chem. Phys.* **1993**, *98*, 1358; *J. Chem. Phys.* **1994**, *100*, 2975.
- (35) Badger, R. M. *J. Chem. Phys.* **1940**, *8*, 288.
- (36) Yates, B. F.; Schaeffer III, H. F.; Lee, T. J.; Rice, J. E. *J. Am. Chem. Soc.* **1988**, *110*, 6327.
- (37) DeTuri, V. F.; Hintz, P. A.; Ervin, K. M. *J. Phys. Chem.* **1997**, *101*, 5969.
- (38) Huisken, F.; Kaloudis, M.; Kulcke, A. *J. Chem. Phys.* **1996**, *104*, 17.
- (39) Ayers, G. P.; Pullin, A. D. E. *Spectrochim. Acta, Part A* **1976**, *32*, 1629.
- (40) Pople, J. A.; *Proc. R. Soc. (London)* **1951**, *205A*, 163.
- (41) Mansky, E. J.; Flannely, M. R. *J. Chem. Phys.* **1993**, *99*, 1962.
- (42) Chalasinski, G.; Szczesniak, M. M.; Scheiner, S. *J. Chem. Phys.* **1991**, *94*, 2807; F.-M. Tao Klemperer, W. *J. Chem. Phys.* **1994**, *101*, 1129.